Taste receptor T1R3 in nasal cilia detects *Staphylococcus aureus* D-amino acids to enhance apical glucose uptake

Ryan M. Carey,[1] Nithin D. Adappa[1], James N. Palmer[1], Noam A. Cohen[1,2], and Robert J. Lee[1,3,4]

[1]Department of Otorhinolaryngology, University of Pennsylvania Perelman School of Medicine
[2]Philadelphia VA Medical Center Surgical Service
[3]Department of Physiology, University of Pennsylvania Perelman School of Medicine
[4]Correspondence to: rjl@pennmedicine.upenn.edu

Running title: T1R3 sweet receptor in airway motile cilia

Abstract

Bitter (T2R) and sweet/umami (T1R) taste receptors serve diverse chemosensory roles all over the body. In airway motile cilia, T2Rs detect bacterial quinolones and lactones to stimulate defensive nitric oxide production. T1Rs in solitary chemosensory (tuft) cells detect glucose in airway surface liquid (ASL) and sweet D-stereoisomer amino acids to regulate antimicrobial peptide secretion. Here, we found that T1R3 is also expressed in human and mouse nasal cell cilia. In differentiated air-liquid interface cultures, T1R3 activation by sucralose lowers ASL glucose, and this is blocked by T1R3 inhibitor lactisole or in *TAS1R3*$^{-/-}$ mice. Activators of T1R3 increase apical glucose uptake, measured using a fluorescent glucose analogue. T1R3 increases expression of GLUT2 and GLUT10, two major apical glucose transporters in airway cells. We found that D-amino acids are produced at low mM concentrations by patient cultures of *Staphylococcus aureus* or S. aureus clinical isolates, while *P. aeruginosa* do not produce D-amino acids. D-amino acids also activate T1R3 and increase GLUT2 and GLUT10 to increase apical glucose uptake and lower ASL glucose. Activation of T1R3 correlated with β-arrestin recruitment to cilia, and an inhibitor of β-arrestin signaling reduced responses observed here. Inhibitors of Ca^{2+}, cAMP, or Rho kinase did not affect T1R3 GLUT2/GLUT10 responses. Our data suggest that T1R3 localized to cilia functions as an immune detector for D-amino acids to reduce ASL glucose through β-arrestin-mediated signal transduction, likely to limit bacterial growth. T1R3 in cilia thus may be a target to modulate ASL glucose in some types of respiratory infections.

Keywords: Staphylococcus aureus, arrestin, glucose transporter, chemosensation, chronic rhinosinusitis, respiratory infections

Introduction

The regulation of airway surface liquid (ASL) glucose is an important component of epithelial innate defense. Despite constant diffusional glucose flux across the airway epithelial barrier from the serosal fluid into the airway lumen,[1-3] ASL glucose is kept ~10-fold lower than serum glucose to limit glucose availability for bacterial growth.[4-6] Airway cells keep the ASL glucose low through apical re-uptake of glucose through glucose transporters, including GLUT2 and/or GLUT10,[7, 8] followed by epithelial metabolism of the glucose.[9] Hyperglycemia can increase the driving force for glucose flux, and inflammation can disrupt tight junctions to increase glucose leak.[7, 10] Both conditions can increase ASL glucose and create a more favorable environment for pathogen growth.[1, 2, 4, 11, 12] We found that patients with chronic rhinosinusitis (CRS) have increased glucose in their nasal secretions compared with control individuals, despite no differences in blood glucose.[13] Elevated ASL glucose in CRS patients is not lowered by corticosteroids,[14] and thus reducing excess nasal fluid glucose may be a beneficial complementary therapeutic strategy even in CRS patients responsive to steroid therapy.

We previously showed that elevated ASL glucose can inhibit innate defense responses mediated by solitary chemosensory cells (SCCs). SCCs are also known as “tuft cells” because of similarities to intestinal tuft cells named for their apical tuft of microvilli. These cells are also referred to as “brush cells.”[15] SCCs regulate several responses, including IL-25 and/or acetylcholine release to activate epithelial inflammation or trigger mucus clearance, respectively.[16, 17] In the nose, they also regulate secretion of antimicrobial peptides like defensins.[13, 18] SCC activation of antimicrobial peptide secretion is reduced by activation of the sweet taste receptor (taste family 1 receptor) subunits T1R2 and T1R3 via ASL glucose[13] or sweet bacterial D-amino acids.[18] While eukaryotes have evolved to use primarily use L-stereoisomer amino acids, many bacteria produce and use D-amino acids.[19, 20] Many D-amino acids activate the sweet taste receptor and thus taste sweet.[21] Both D-Phe and D-Ile produced by Staphylococcus aureus can activate SCC sweet taste receptors and inhibit antimicrobial peptide release in primary nasal cells *in vitro*.[18]

A previous study of rat tracheal epithelium suggested that the T1R3 sweet taste receptor subunit is also expressed in multi-ciliated cells as well as SCCs.[22] This study showed that T1R3 was co-expressed in cells with GLUT2, and thus the authors hypothesized that T1R3 in ciliated cells may play a role in glucose transport. Because of the role of ASL glucose regulation in immune defense, we hypothesized that T1R3 in airway cilia may function in part to sense “sweet” bacterial metabolites like D-amino acids to increase glucose uptake and reduce pathogen growth.

Airway motile cilia are critical to clear the respiratory tract of inhaled particulates and pathogens that get trapped in airway mucus on top of the ASL.[23] Coordinated beating of cilia transports mucus to the oropharynx, where it is expectorated or swallowed. More recently, airway motile cilia have also

been identified as chemosensory organelles important in cell signaling[24-26] In nasal epithelial cells, bitter taste receptors (taste family 2 receptors or T2Rs) in airway cilia detect bitter bacterial lactones and quinolones to activate nitric oxide production to clear and kill bacteria.[27-29] Here, we sought to determine if human nasal epithelial cells express the T1R3 sweet taste receptor subunit within motile cilia, and if this receptor regulates glucose transport in response to bacterial D-amino acids. The sweet taste receptor is highly druggable via artificial sweetener agonists[30, 31] or antagonists like lactisole[32] or gymnemic acid,[33] many of which are already approved for ingestion and could be delivered via topical nasal rinse.[34] We thus hypothesize that the sweet taste receptor may be a logistically feasible target for altering nasal epithelial glucose concentrations in some CRS patients.

Results

T1R3 expression and localization to motile cilia and negative regulation by TLR5

T1R3 expression was detected by immunofluorescence and laser scanning confocal microscopy in motile cilia of differentiated air-liquid interface (ALI) cultures, co-labeled with β-tubulin IV-directed primary antibody (**Figure 1A**) using rabbit serum as a non-specific binding control (**Figure 1B**). While we previously published evidence of T1R3 expression in SCCs,[13, 18] the cilia-localized T1R3 was not apparent at first, because cilia are more difficult to permeabilize. For IF of SCCs, we typically utilize gentler permeabilization (0.1% triton, 10 min) than for cilia (0.3% triton, 1 hour), as cilia are covered with cell attached mucins which make permeabilization difficult. Orthogonal slices confirmed expression of T1R3 the level of cilia (βTubIV) above the level of phalloidin, which stains the actin-enriched microvilli at the base of the cilia (**Figure 1C**). Direct primary antibody labelling showed co-overlapping staining of two different T1R3 rabbit-raised polyclonal antibodies (**Figure 1D**). Cilia staining with a goat-raised T1R3 antibody was reduced by an antigenic blocking peptide (**Figure 1E**). Similar staining was observed in whole mount fresh nasal tissue using a rabbit-raised polyclonal antibody(**Figure 1F**). Finally, we observed cilia staining with a mouse T1R3-directed rabbit polyclonal antibody in mouse nasal septal ALIs, and this staining was absent in ALIs derived from tissue from T1R3 knockout (*TAS1R3*$^{-/-}$) mice (**Figure 1G**).

We saw an increase in *TAS1R3* gene transcript by qPCR as primary nasal cells were differentiated at ALI (**Figure 2A**), as observed with cilia-expressed *TAS2R* bitter receptor genes.[29] Goblet-cell MUC5AC and cilia-localized MS4A8B[35] were used as controls. As we previously observed with several bitter receptors,[29] *TAS1R3* transcript was reduced by airway cell stimulation with toll-like receptor 5 (TLR5) agonist *Pseudomonas aeruginosa* flagellin (**Figure 2B**). Both *TAS1R3* decrease and *CXCL8* (*IL-8*) increase were reduced by addition of soluble TLR5 ectodomain (**Figure 2B-D**), supporting this was indeed due to flagellin that was scavenged by the soluble TLR5. Moreover, conditioned media from bacteria isolated from three CRS patients with confirmed *P. aeruginosa* infections likewise decreased *TAS1R3* expression in primary nasal ALIs (**Figure 2D**). Together, these data suggest that T1R3 is expressed in nasal cilia, and *TAS1R3* transcript is negatively regulated by TLR5 signaling, much like the cilia-localized T2Rs.[29]

T1R3 modulates airway surface liquid glucose

As described in the introduction, ASL glucose is a balance of glucose leak and glucose re-uptake by epithelial cells. When cultured at ALI, cell lines like RPMI2650 or A549 that form less of a tight junction barrier (evidenced by lower transepithelial electrical resistance [TEER]; **Figure 3A**) than primary nasal cells are less able to keep ASL glucose concentrations low during acute (18 hr) challenge

with high glucose (**Figure 3B**). We noted that, in the presence of high basolateral glucose (10 or 15 mM), primary nasal cells also exhibit increased ASL glucose in the presence of T1R3 allosteric inhibitor lactisole (2 mM; apical side only; 18 hrs.) [31, 32] and lower ASL glucose in the presence of non-metabolizable T1R3 agonist sucralose (2 mM; apical side only; 18 hrs) (**Figure 3C**). There was no change in TEER (**Figure 3D**) or *CXCL8*/*IL8* transcription (**Figure 3E**), suggesting no changes in barrier function or inflammatory state of the cells with sucralose or lactisole treatment.

We tested the role of T1R3 in this observation using mouse nasal septal cells grown at ALI from Wt or T1R3 knockout (*TAS1R3*$^{-/-}$) mice.[36] Sucralose decreased ASL glucose in Wt but not *TAS1R3*$^{-/-}$ mice in the presence of 15 mM basolateral glucose (**Figure 3F**). Because we had shown that T1R3 functions in solitary chemosensory cells, which utilize Gα-gustducin (GNAT3), we also tested this response in cells from Gα-gustducin knockout mice (*GNAT3*$^{-/-}$) mice and saw no loss of this sucralose effect (**Figure 3F**), suggesting it is Gα-gustducin-independent.

We hypothesized that a function of T1Rs in airway cilia might be to detect bacterial D-amino acids. Certain D-stereoisomer amino acids have been identified as "sweet" in psychophysics studies[37, 38] and demonstrated to activate the T1R2/3 heterodimer in molecular experiments.[21, 31] It is important to note here that, while we are using the term "sweet," responses here are distinct from the gustatory sensation of sweetness. We are using this term to refer to activation of the T1R2/3 heterodimer and/or T1R3 homodimer receptors, not the psychophysical perception of taste. To confirm our prior observation[18] that D-amino acids are present in conditioned media (CM) from patient bacteria composed predominately of *Staphylococcus*, we tested a fluorometric assay that can detect D-amino acids but not their L-isomers (**Figure 4A**). We found that CM from clinical and lab (strain M2[39]) *Staphylococcus aureus* and a clinical strain of *Staphylococcus epidermidis* had D-amino acids present. Media from clinical and lab (PAO-1) *P. aeruginosa* strains did not (**Figure 4B**). The D-amino acid content we saw in Staphylococcus CM (>1 mM) is similar to the value of ~1.5 mM previously reported for *S. aureus* media.[40] When we looked at CM from sinonasal clinical cultures, we saw D-amino acids present in cultures in which *S. aureus* was predominant but not CM from cultures in which *P. aeruginosa* was predominant (**Figure 4C**). Because these samples came from human patients, they were not strictly single-species cultures but were classified based on the predominant microorganisms present in each culture, as previously described.[18] Other species were also likely present in each culture at lower abundance.

Sweet D-amino acids D-Phe, D-Leu, and D-Trp reduced ASL glucose in primary nasal ALIs in the presence of 15 mM basolateral glucose (**Figure 5A**). This effect was reduced in the presence of lactisole (**Figure 5B**). We also saw lowering of ASL glucose with CM from patients infected with *S. aureus* but not with CM from patients with *P. aeruginosa* (**Figure 5C**). Again, this did not occur in the

presence of lactisole (**Figure 5D**). Together, these data suggest *S. aureus* D-amino acids might reduce ASL glucose by interacting with T1R3.

T1R3 enhances apical glucose uptake

To measure glucose uptake, we utilized a fluorescent derivative of D-glucose, 2-[N-(7-nitrobenz-2-oxa-1, 3-diazol-4-yl)amino]-2-deoxy-d-glucose (2-NBDG). NBDG is transported by most diffusional (GLUT) and sodium linked (SGLT) glucose transporters studied, albeit possibly with slightly altered kinetics.[41, 42] We used NBDG (200 μM) on the apical side only of cultures to preferentially measure cellular uptake from the apical side of the epithelial barrier. We quantified uptake over 70 min of exposure to NBDG (**Figure 6A**) after 18 hours of exposure to apical PBS (control) or PBS with lactisole or sucralose (2 mM each). Prior apical sucralose increased NBDG uptake while lactisole reduced it (**Figure 6A-B**) Acute addition of GLUT inhibitor phloretin (200 μM) or 15 mM glucose to outcompete the NBDG reduced NBDG uptake (**Figure 6A-B**). Use of Na^+-free (0-Na^+) PBS had no effect, suggesting NBDG transport is not Na^+-linked (e.g., SGLT-mediated). GLUT1-specific inhibitor STF-1 (100 μM) had no effect, suggesting the phloretin inhibition was not through GLUT1 (**Figure 6B**). We also saw an increase in NBDG uptake after 18 hours exposure to D-amino acids in the absence but not presence of lactisole (**Figure 6C-D**). L-amino acids had no affect (**Figure 6C**). Prior exposure to CM from patients with *S. aureus* also increased NBDG uptake compared with media only control (**Figure 6E**), and this was reduced in the presence of lactisole (**Figure 6D**). CM from *P. aeruginosa* patients had no effect on NBDG uptake (**Figure 6E**).

To confirm a role for T1R3, we again utilized cells from *TAS1R3*$^{-/-}$ knockout mice, grown at ALI. There was no increase in NBDG uptake with prior (18 hrs) sucralose treatment in *TAS1R3*$^{-/-}$ ALIs (**Figure 6F-G**). In contrast, both Wt and GNAT3$^{-/-}$ ALIs exhibited an increase in NBDG uptake after sucralose pretreatment (**Figure 6F-G**). When NBDG was placed on the basolateral side of cultures, there was no increase in NBDG uptake with sucralose or sweet amino acid D-Trp (**Figure 6H**). Thus, the effects described above are specific for the apical membrane of the epithelium.

To further test if this is an effect that occurs within ciliated cells or if this requires solitary chemosensory cells, we took cells acutely isolated from mouse nasal turbinate expressing GFP under a TRPM5 promotor,[43] which labels solitary chemosensory cells as well as taste cells.[13, 44] We used lack of GFP fluorescence to confirm the absence of solitary chemosensory cells in epithelial clumps. We observed a sucralose-mediated NBDG uptake increase in these cell clumps (**Figure 6I**), suggesting the responses we observed are independent of solitary chemosensory cells. Lactisole was not used here as it does not bind to mouse T1R3.[32]

Finally, to confirm the results above with a more physiological assay, we imaged NAD(P)H autofluorescence upon addition of apical glucose after 24 hrs exposure to sucralose ± lactisole ± phloretin. NADH and NADPH, but not NAD and NADP, are autofluorescent when excited by UV light, and addition of metabolites to cells can sometimes be visualized by increases in NAD(P)H production and increases in autofluorescence.[45, 46] Our goal here was not to perform a rigorous metabolic characterization, but rather to test if changes in metabolism could be observed along with the changes in NBDG transport already described. We observed that NAD(P)H autofluorescence increased faster in response to introduction of 5 mM apical glucose cultures pretreated with sucralose and slower in cultures pre-treated with lactisole compared with control cultures (**Figure 6J**). Acute application of GLUT inhibitor phloretin reduced the autofluorescence increase seen with sucralose (**Figure 6J**). These data support the NGDG data suggesting nasal epithelial cells are taking up glucose faster across the apical membrane after pretreatment with sucralose in a lactisole-sensitive fashion. This supports a role for T1R3 in ASL glucose regulation by modifying apical glucose uptake.

T1R3 increases expression of GLUT2 and GLUT10, likely via arrestin signaling

The major GLUT transporters reported for airway epithelial cells are GLUT2 and GLUT10 on the apical side and GLUT1 on the basolateral side.[2, 7] While one study reported apical GLUT4 in airway epithelial cells, we did not see substantial GLUT4 transcript expression in nasal ALIs compared with other GLUTs (**Figure 7A**). Publicly available gene expression data also suggest GLUT1 and GLUT10 are the predominant GLUT isoforms in bronchial and nasal cells, with no significant differences in expression with mucociliary differentiation, cigarette smoking, or cystic fibrosis (**Supplemental Figure 1**). Thus, we focused largely on GLUT1, GLUT2, and GLUT10 for these studies. Human GLUT10 is a high affinity glucose transporter with K_m of ~0.3 mM,[47-49] fitting with a potential role in keeping nasal ASL glucose as low as possible, normally ~0.5 mM or ~10-fold below normal serum levels of ~5 mM.

Sucralose (2 mM; apical side only; 18 hrs;) increased transcript levels of GLUT2 and GLUT10, while GLUT1 transcript was unaltered (**Figure 7A**). The sucrose-induced change in GLUT2 and GLUT10 was blocked by lactisole (2 mM; apical side only; **Figure 7A**). We also observed that sucralose increased GLUT2 immunofluorescence at the apical membrane, identified by microvilli marker ezrin (**Figure 7B-C**). This was also blocked by lactisole (**Figure 7B-C**). Like sucralose, sweet D-amino acids D-Phe, D-Ile, or D-Trp (2 mM; apical side only; 18 hrs) increased GLUT2 and GLUT10 in a lactisole-dependent manner (**Figure 7D-E**). The effects of D-Phe were reduced in cultures pre-treated with flagellin (**Figure 7F**), which reduces T1R3 expression. These data suggest the apical glucose uptake results observed above are partly due to GLUT2 and GLUT10 increase.

How does this occur? We previously showed no effect of sucralose on Ca^{2+} signaling, NO production, or ciliary beat frequency in nasal epithelial cells.[13, 50] We hypothesized the changes in gene expression may occur through arrestin-dependent or independent kinase signaling. While kinase signaling downstream of taste receptors is grossly understudied, sucralose was previously shown to signal through ERK1/2 in Min6 cells.[51] We examined primary nasal ALIs after 1 hour of sucralose, D-Phe, or D-Ala stimulation. Cells were fixed and stained with a pan-β-arrestin antibody. We visualized more intense arrestin localization in cilia with stimulation of sucralose, D-Phe, or D-Ala, and this was blocked by lactisole (**Figure 8A-B**). Arrestin inhibitor barbadin[52] reduced GLUT2 and GLUT10 expression increases in response to 18 hrs. sucralose, D-Phe, or D-Ala (**Figure 8C**). No inhibition was observed with phospholipase C inhibitor U73122 (1 μM), $G\alpha_i$ inhibitor pertussis toxin (10 ng/ml), or rho-kinase inhibitor Y-27632 (1 μM) (**Figure 8D**), suggesting cilia T1R3 responses are independent of G protein signaling and perhaps tied to arrestin-mediated kinase signaling.

Discussion

Here we show that T1R3 expressed in nasal epithelial cilia detects bacterial sweet D-amino acids and regulates expression of glucose transporters GLUT2 and GLUT10, likely through a β arrestin-dependent pathway. On the tongue, the sweet taste receptor is a heterodimer of T1R2 and T1R3.[53-55] It still needs to be determined if T1R2 and/or umami receptor subunit T1R1 play a role in the airway cilia response observed here. T1R3 homodimers have been suggested to function in pancreatic beta cells,[56-58] which could also be the case here. Future work is needed, partially limited by the availability of reliable T1R antibodies. The use of T1R3 knockout mice and T1R3 antagonist lactisole in this study was critical to rigorously determining a role for T1R3 here.

While the exact mechanism(s) of the T1R3 signaling to regulate GLUT2/GLUT10 expression changes remain to be determined, the data here suggest it might be independent of G protein signaling and instead dependent on arrestin-mediated kinase signaling. Further work is needed to explore the relatively unknown non-G-protein arms of taste receptor signaling. Our work also suggests that airway motile cilia chemosensation likely involves more than just the cAMP and Ca^{2+} pathways previously implicated in the signaling from these organelles,[24, 25] further blurring the lines between motile and primary (sensory) cilia.

We hypothesize that a sweet agonist (artificial sweetener), delivered via topical nasal rinse, might reduce ASL glucose. The identity of the potential agonists to use partly depends on whether other T1R isoforms are expressed. While sugars like sucrose and glucose likely bind to the extracellular venus fly trap domains of both T1R2 and T1R3[59-61] the some artificial sweeteners like aspartame[31, 62, 63] and xylitol[64] bind to T1R2 while others like cyclamate bind T1R3.[30] Future screening is needed to determine the most efficacious sweet agonists, which could make use of the differentiated human nasal ALI model used here. Mice have reduced ability to detect some artificial sweeteners due to sequence differences between human and mouse T1R2,[62, 65] possibly precluding use of mice as a preclinical screening model. Likewise differences in T1R3 sequences cause antagonist lactisole to not bind to mouse T1R3.[32] While our data suggest mechanistic studies might be done in mice, drug screening studies should employ human cells, as with bitter taste receptors.[66]

It also remains to be determined if this is truly a *bona fide* defensive response to limit all pathogen growth or a more subtle way to change the ASL to a more friendly environment for some bacteria and less friendly environment for others. Glucose is an excellent carbon sources for many bacteria, including *Staphylococcus* gram-positive species and gram-negatives like *Escherichia coli* and *P. aeruginosa*.[67, 68] However, *E. coli* and *P. aeruginosa* may grow better in high glucose conditions than *Staphylococcus aureus* and commensal *Staphylococcus epidermidis*.[69] The downregulation of this T1R3 cilia pathway by *P. aeruginosa* flagellin-TLR5 signaling (reducing T1R3 ASL glucose

regulation) and converse activation of the T1R3 cilia pathway by *S. aureus* D-amino acids suggests that bacteria can differentially modulate this pathway. Whether this is host-pathogen or host-commensal/host-microbiome crosstalk remains to be elucidated. It might be both, determined by the level of the relative stimuli the host cell receives.

One question that arises is whether the inhibition of SCCs expected to occur with a topically delivered sweet agonist might be detrimental despite activation of T1R3 in cilia reducing airway glucose. This may indeed be the case. Further investigation is needed. However, SCCs do not appear to be as common in the human airway as in mice, though detailed rigorous studies of SCC presence and localization in the human airways are still to be undertaken. SCCs appear to be regulated by type II cytokines like IL-13 or IL-4 and/or exposure to fungal metabolites.[16] Thus, SCCs may only be prevalent in the nose of CRS patients with nasal polyps (CRSwNP), a subset of CRS driven by type II cytokines,[70] or in patients with allergic fungal sinusitis. CRS without (*sans*) nasal polyps (CRSsNP) is most often characterized by other inflammatory profiles.[70] We might find that sweet agonists are useful in CRSsNP but not CRSwNP. Or, when activating T1Rs to reduce ASL glucose, the associated suppression of SCCs in CRSwNP may also suppress SCC IL-25 generation, reduce inflammation, and still be beneficial despite suppression of antimicrobial production. Our data here reveal cilia T1R3 as a novel regulator of ASL glucose that might be pharmacologically leveraged in CRS or other airway diseases. However, determining how cilia T1R3 fits into the context of these diseases will require several more *in vivo*-focused studies.

Methods

Reagents

Anti-human T1R3 PA5-34256 (rabbit polyclonal), β-arrestin1/2 antibody PA1-730 (rabbit polyclonal), and ezrin 3C12/MA5-13862 (mouse monoclonal) antibodies were from ThermoFisher Scientific. Anti-human T1R3 SAB4503300 (rabbit polyclonal) and acetylated tubulin T7451 (mouse monoclonal) antibodies were from Sigma. Anti-human T1R3 ab150525 (rabbit polyclonal) and beta-tubulin IV ab11315 (mouse monoclonal) antibodies were from Abcam. Anti-mouse T1R3 NB100-98792 (rabbit polyclonal) was from Novus. Anti-human T1R3 MBS421865 (goat polyclonal) and blocking peptide MBS428461 were from MyBioSource. Lactisole, U73122, pertussis toxin, sucralose, 2-NBDG, and D-amino acids were from Cayman Chemical. Fluorometric D-amino acid kit (ab239721) was from Abcam. Unless indicated all other reagents were from Sigma. *P. aeruginosa* flagellin (FLA-PA) and soluble TLR5 ectodomain (hTLR5-Fc) were from InvivoGen. Dulbecco's phosphate buffered saline (DPBS) contained (in mM) 138 NaCl, 2.7 KCl, 1.5 KH_2PO_4, 8 Na_2HPO_4, 1.8 $CaCl_2$, and 1.5 $MgCl_2$, with pH adjusted to approximately 7.2. Glucose was added to this solution when indicated in the text. Isosmotic substitution of N-Methyl-D-Glucamine-Cl for NaCl was used to make Na^+-free (0-Na^+) PBS. For all assays, basolateral media was changed to phenol-free glucose-free Dulbecco's modified Eagle's medium (DMEM; Gibco/ThermoFisher Scientific) plus 2% NuSerum (Corning) and glucose added to the indicated basolateral concentrations.

Cell culture

Immortalized cells (RPMI2650 and A549) were obtained from ATCC and grown in minimal essential media (MEM; Gibco/ThermoFisher Scientific) plus 1x cell culture penicillin/streptomycin and 10% FetalPlex serum substitute (Gemini Biosciences). For air-liquid interface (ALI) cultures, cells were seeded onto collagen-coated 0.33 cm^2 transwell filters (Corning) and grown to confluence for 5 days before apical air exposure, as described previously [71, 72] Cultured cells were used after 10-14 days at ALI. TEER was measured using an epithelial volt-ohm meter (EVOM; World Precision Instruments) and chopstick electrodes.

Primary human nasal surgical specimens were obtained according to The University of Pennsylvania guidelines for use of residual clinical material from patients undergoing sinonasal surgery at the Hospital of the University of Pennsylvania with institutional review board approval (#800614). Written informed consent was obtained from patients in accordance with the U.S. Department of Health and Human Services code of federal regulation Title 45 CFR 46.116. Patients ≥18 years of age requiring surgery for sinonasal disease or trans-nasal approaches to the skull base were included.

Patients systemic inheritable disease (eg, granulomatosis with polyangiitis, systemic immunodeficiencies) or those using antibiotics, oral corticosteroids, or anti-biologics (e.g. Xolair) within one month of surgery were excluded. Vulnerable populations (patients ≤18 years of age, pregnant women, and cognitively impaired persons) were also excluded.

Mucosal tissue transported to the lab on ice in saline for subsequent enzymatic dissociation. Cells were grown to confluence in proliferation medium (7 days), then lifted and seeded at high density on transwells (Corning transparent, 0.33 cm^2, 0.4 μm pore size) as described [50, 72-74]. The next day, basolateral media was changed to differentiation medium and culture medium was removed from the upper compartment. Differentiation media contained 1:1 Lonza bronchial epithelial cell basal media (BEBM):Dulbecco's modified Eagle's medium (DMEM) plus Lonza singlequot supplements (0.5 ng/ml hEGF, 5 ng/ml epinephrine, 0.13 mg/ml BPE, 0.5 ng/ml hydrocortisone, 5 ng/ml insulin, 6.5 ng/ml triiodothyronine, and 0.5 ng/ml transferrin, 0.1 nM retinoic acid) supplemented with 1x penicillin/streptomycin and 2% NuSerum (BD Biosciences/Corning, San Jose, CA) as described.[50] Cells were fed from the basolateral side only with differentiation media for ~21-28 days before use.

Mouse nasal septal ALI cultures were grown as described[75] from residual tissue from animals sacrificed for other experimental purposes with IACUC approval. No mice were sacrificed for the purposes of this study. Epithelial cells were isolated by collagenase and pronase digestion before culture on Costar 6.5 mm transwell permeable filter supports (Corning Inc. Life Sciences, Lowell, MA USA) with apical side submerged. After 7 days, cells reached confluence and the medium was removed from the apical surface with feeding from the basolateral side. Differentiation and ciliogenesis were observed within 10–14 days after exposure to air, and cultures were used within 4–6 weeks.

Immunofluorescence microscopy.

Immunofluorescence staining for cilia was carried out as described.[50, 72, 74] ALI cultures were fixed in 4% formaldehyde for 20 min at room temperature, followed by blocking and permeabilization for 1 hour at 4°C in Dulbecco's phosphate buffered saline (DPBS) containing 1% bovine serum albumin (BSA) plus 5% normal donkey serum (NDS) to block non-specific protein binding and 0.2% saponin plus 0.3% Triton X-100 to permeabilize. After three washes (5 min each) in DPBS, primary antibody incubation (1:100) was performed in DPBS containing BSA, NDS, and saponin overnight at 4°C. After another round of washing in DPBS, incubation with AlexaFluor (AF)-conjugated donkey anti-mouse or anti-rabbit secondary antibodies (1:1000; ThermoFisher Scientific) was performed at 4°C for 2 hours in DPBS plus BSA, NDS, and saponin.

After staining, transwell filters were removed from plastic retaining rings and mounted onto slides with Fluoroshield + DAPI mounting media (Abcam; Cambridge, MA USA). For co-staining with

direct labeling of primary antibodies, Zenon antibody labeling kits (Thermo Fisher Scientific) for AF546 or AF647 were used as described.[50, 72, 74] In some experiments, images of ALIs were taken on an Olympus Fluoview confocal system with IX-73 microscope and 60x (1.4 NA) objective. For other experiments, images were taken on an Olympus IX-83 microscope with spinning disk confocal unit (Olympus DSU) with 60x (1.4 NA) objective using Metamorph. All images were analyzed in FIJI [76] using only linear adjustments (min and max), set equally between compared images obtained at identical microscope settings (exposure, objective, binning, etc.).

ASL glucose measurements

ASL glucose concentrations were measured as previously described.[13] ALI cultures were transferred to 5 mM glucose (minimal essential media + Earl's salts + 1% NuSerum) for 24 hrs. Basolateral glucose was then changed to the values indicated in the text, and 30 µl PBS was placed on the apical side of the ALIs for 24 hours, assuming that glucose concentration would equilibrate over this time and reflect the physiological ASL concentrations generated by these cultures. Apical samples were collected and run on a colormetric glucose assay (Cayman Chemical) using manufacturer-provided glucose standards.

NBD-glucose uptake

2-NBDG in PBS was incubated on the apical side of cultures at the concentrations and times indicated in the text. Followed by incubation, cells were copiously washed with NBDG-free PBS and immediately imaged in the center of the culture using standard FITC filter set on an Olympus IX83 microscope with 4x 0.16NA objective and Metamorph (Molecular Devices). Images were taken at exactly the same microscope settings with no nonlinear adjustments.

NAD(P)H autofluorescence

NAD(P)H autofluorescence[45, 46] was imaged as described.[77] We excited ALIs with a Xenon lamp (Sutter Lamda LS 300 W) with high UV output at 340 nm and measured fluorescence at 450 nm using a DAPI filter set and 30x 1.0 NA silicone oil immersion objective lens with high UV transmittance on an IX-83 microscope (Olympus) equipped with a Hammamatsu Orca Flash 4.0 sCMOS camera (Hammamatsu, Tokyo, Japan). Images were acquired every 12 seconds using Metafluor (Molecular Devices, Sunnyvale CA). Transwells with no cells were used to subtract background from plastic autofluorescence. Cultures were kept in 5 mM basolateral glucose, and apical surface contained 30 µL of 0-glucose PBS. Apical glucose was changed from 0 mM to 5 mM by subsequent addition of an equal volume of PBS supplemented with 10 mM glucose.

Quantitative reverse-transcription PCR (qPCR)

Quantitative reverse transcription PCR (qPCR) was carried out as described.[29, 78] ALIs were lysed in TRIzol (ThermoFisher) and RNA was isolated using Direct-zol (Zymo Research). cDNA was transcribed via High-Capacity cDNA Reverse Transcription Kit (ThermoFisher) and gene expression was quantified utilizing Taqman qPCR probes and QuantStudio 5 Real-Time PCR System (ThermoFisher). Data were analyzed using Excel and GraphPad PRISM. UBC was used as a housekeeping control gene as described.[29, 78]

Microbiological cultures

Patient sinonasal microbiology cultures were collected from sinonasal swabs using BBL CultureSwab Plus transport system (Becton, Dickinson, and Co., Sparks MD USA), grown overnight in lysogeny broth (LB) media for 24 hrs at 37 °C, followed by freezing of glycerol stocks and speciation by the Philadelphia VA Medical Center microbiological laboratory (Dr. L. Chandler). Conditioned media was obtained from subsequent 24 hr overnight cultures normalized by diluting turbidity to 0.5 MacFarland and filtering through a 0.2 µm filter. Sweet D-amino acid production was previously demonstrated from the *Staphylococcus* patient CMs used here via liquid chromatography and tandem mass spectrometry (LC-MS/MS).[18] This was confirmed by D-amino acid assay used here.

Data analysis and statistics

Numerical data were compiled in Excel (Microsoft) and graphed in Prism (GraphPad software, La Jolla, CA). All data in bar graphs are shown as mean ± SEM. Statistical analyses of multiple comparisons were made in Prism using one-way ANOVA with Bonferroni (pre-selected pairwise comparisons) or Dunnett's (comparing to control value) post-tests; $p < 0.05$ was considered statistically significant. Asterisks (* and **) indicate $p < 0.05$ and $p < 0.01$, respectively. Raw data points used to construct graphs or traces are available upon request.

Acknowledgements: The authors thank M. Victoria, L.E. Kuek, J.R. Freund, B.M. Hariri, and B. Chen (University of Pennsylvania) as well as G. Xiong (Children's Hospital of Philadelphia) for technical assistance and helpful discussions. We thank R. Margolskee (Monell Chemical Senses Center) for access to *TAS1R3*$^{-/-}$, *GNAT3*$^{-/-}$, and TRPM5-GFP mouse tissue. We thank Dr. L. Chandler (Philadelphia VA Medical Center) for microbiology assistance and isolation of clinical strains. This study was supported by NIH/NIDCD grant R01DC016309 to R.J.L. and a pilot project from the Penn Diabetes Research Center supported through NIH/NIDDK grant P30DK19525.

CRediT authorship contribution statement: Ryan M. Carey: Resources, Conceptualization, Data Writing – original draft, Writing – review & editing. Nithin D. Adappa: Resources, Data curation, Project administration, Writing – review & editing. James N. Palmer: Resources, Data curation, Project administration, Writing – review & editing. Noam A. Cohen: Resources, Conceptualization, Data curation, Project administration, Writing – review & editing. Robert J. Lee: Conceptualization, Investigation, Methodology, Formal analysis, Writing – original draft, Writing – review & editing, Project administration.

Declaration of Competing Interest: The authors declare no competing interests.

Data Availability: All materials and data will be provided upon request to the corresponding author

Figure 1

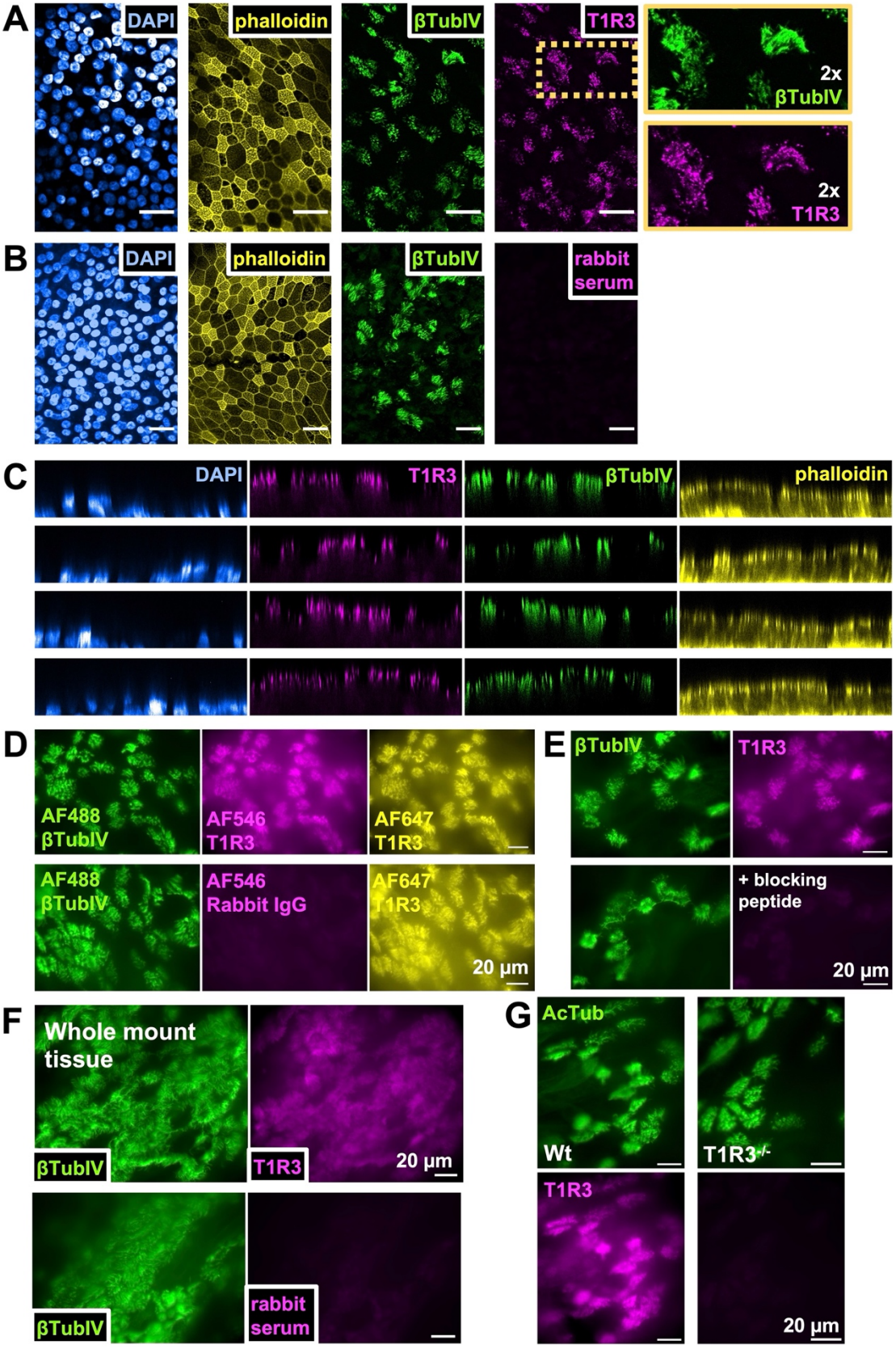
A
DAPI
phalloidin
βTublV
T1R3
2x βTublV
2x T1R3
B
DAPI
phalloidin
βTublV
rabbit serum
C
DAPI
T1R3
βTublV
phalloidin
D
AF488 βTublV
AF546 T1R3
AF647 T1R3
AF488 βTublV
AF546 Rabbit IgG
AF647 T1R3
20 µm
E
βTublV
T1R3
+ blocking peptide
20 µm
F
Whole mount tissue
βTublV
T1R3
20 µm
βTublV
rabbit serum
G
AcTub
Wt
T1R3-/-
T1R3
20 µm

Figure 1. T1R3 localization to nasal epithelial cilia. (A) Laser-scanning confocal micrographs of immunofluorescence of T1R3 (magenta) and β-tubulin IV (green) taken at the same plane. Phalloidin (taken at a plane just below the cilia; yellow) and DAPI (nuclear stain; blue; taken at a plane lower than the phalloidin) shown as control for epithelial integrity. Boxes on the very right shows region outlined in orange at 2x to show co-localization of T1R3 and β-tubulin IV. **(B)** Control staining with rabbit serum showed no cilia labeling. **(C)** Orthogonal slices (*xz*) from immunostaining experiments as in *A* showing the co-localization of T1R3 (magenta) and β-tubulin IV (green) above the level of the phalloidin (yellow). Antibody used in *A* and *C* was Abcam ab150525. **(D)** Direct labeling with AlexaFluor Zenon labeling kits allowed co-staining with AF546-labeled anti-T1R3 (PA5-34256; ThermoFisher; magenta) and AF647-labeled anti-T1R3 (SAB4503300; Sigma; yellow), which both showed co-labeling of cilia (β-tubulin IV; green). Labeling of Rabbit IgG control with AF546 showed no fluorescence of cilia. **(E)** Cilia staining with another T1R3 antibody (MBS421865; MyBioSource) was reduced by its antigenic blocking peptide (10-fold molar excess; 1 hour pre-incubation). Results in A-E representative of staining observed in n = 3 ALIs from individual patients. **(F)** Cilia-staining of T1R3 (ab150525) in thin mucosal tissue pieces acutely removed during sinus surgery. Results representative of staining observed in tissue from n = 3 from individual patients. **(G)** A mouse-directed T1R3 antibody (NB100-98792) stained cilia in ALIs derived from Wt mouse nasal septum but not ALIs derived from *TAS1R3*$^{-/-}$ mouse septum. Results representative of n = 3 from ALIs from each genotype.

Figure 2

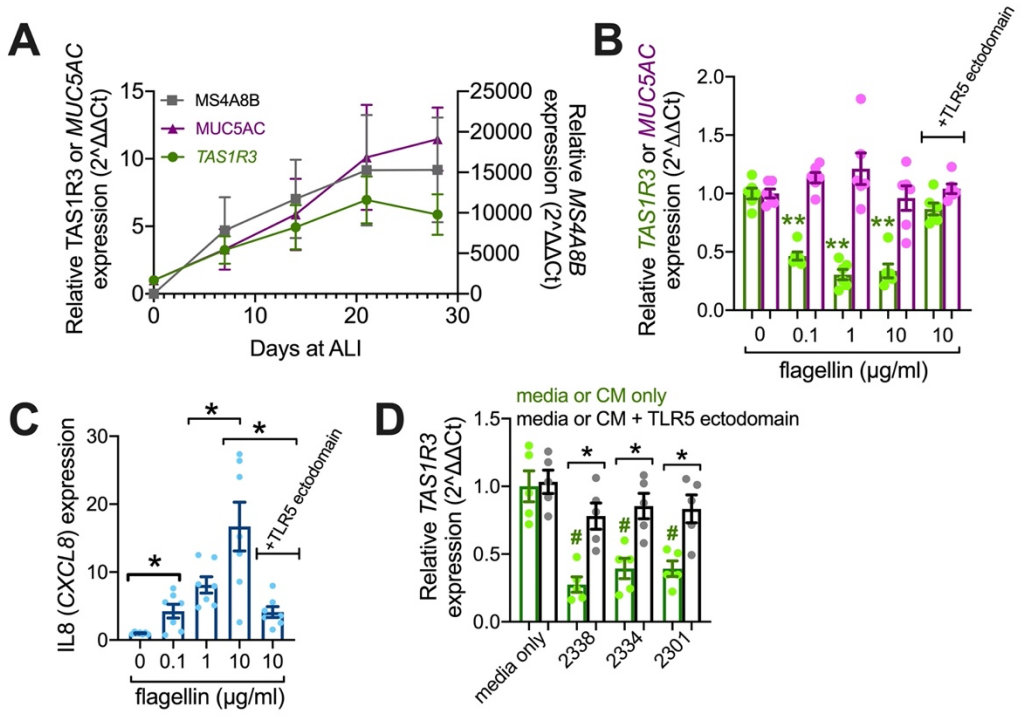

Figure 2. *TAS1R3* mRNA expression in human nasal ALI cultures. (A) Graph showing expression of *TAS1R3* (green), goblet cell marker *MUC5AC* (magenta), and cilia marker *MS4A8B* by qPCR at time points after exposure of ALIs to air. **(B-C)** Bar graphs showing *TAS1R3* (green; *B*) and *MUC5AC* (pink; *B*) or *IL8* (*CXCL8;* blue; *C*) expression in day 21 ALIs ± TLR5 agonist flagellin ± soluble TLR5 ectodomain antagonist. **(D)** Graph showing *TAS1R3* expression after exposure to conditioned media (CM) from patients with *P. aeruginosa* respiratory infections ± TLR5 ectodomain. All data are presented as mean ± SEM using ALIs from n = 6 (*A* and *B*), 7 (*C*), or 5 (*D*) patients in independent experiments. Significances in *B-D* determined by one way ANOVA with Bonferroni posttest; *p<0.05.

Figure 3

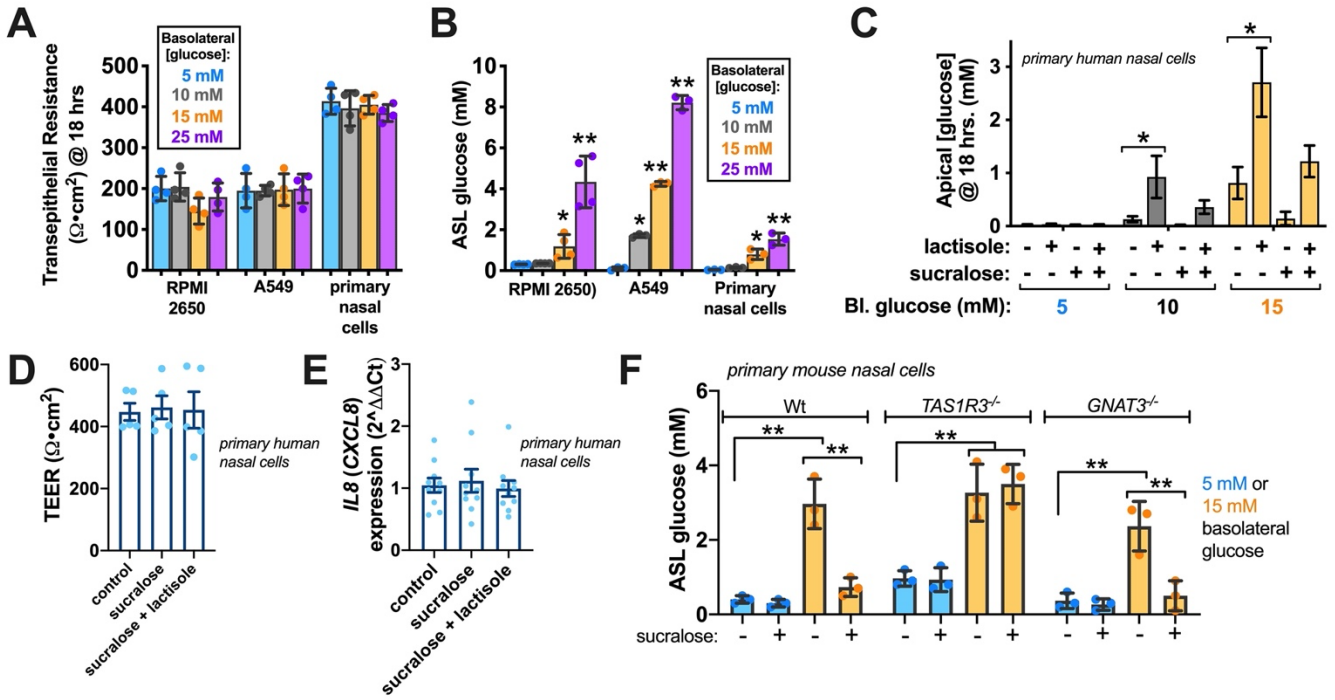

Figure 3. T1R3 participates in airway surface liquid (ASL) glucose regulation. (A-B) Bar graph showing transepithelial resistance (TEER; *A*) and apical glucose concentrations (*B*) of ALI cultures grown from cell lines (RPMI2650, A549) or primary nasal epithelial cells after incubation in 5, 10, 15, and 25 mM glucose; n = 4 independent experiments per condition, primary cells utilized ALIs from 4 individual patients. **(C)** Bar graph showing changes in apical glucose concentrations with elevations of basolateral glucose ± sucralose ± lactisole; n = 3 ALIs from 3 individual patients used per condition in independent experiments. **(D)** Graph showing no change in TEER with sucralose or lactisole (n = 5 ALIs from 5 different patients per condition in independent experiments). **(E)** Graph showing no change in *IL8/CXCL8* expression with sucralose or lactisole (n = 10 ALIs from 10 different patients per condition in independent experiments). **(F)** Experiment similar to *C* but using only sucralose in ALIs grown from Wt, *TAS1R3*$^{-/-}$, or *GNAT3*$^{-/-}$ knockout mice. The ability of sucralose to reduce ASL glucose was lost in *TAS1R3*$^{-/-}$ mice; n = 3 ALIs per condition in independent experiments. All data presented as mean ± SEM. Significances in *B*, C, *D, and F* determined by one way ANOVA with Bonferroni posttest; *p<0.05. *D* and *E* not significant by one way ANOVA.

Figure 4

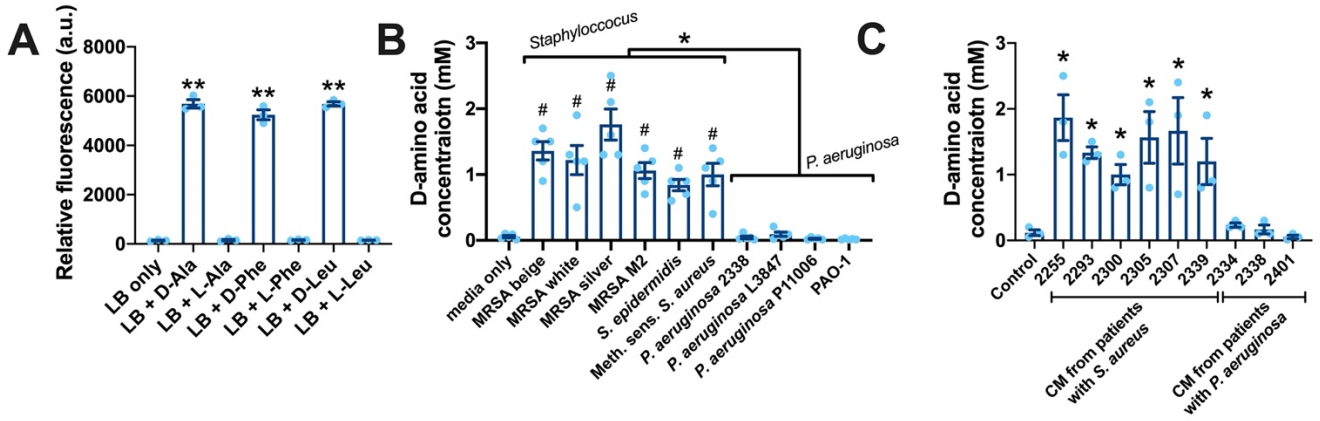

Figure 4. Production of D-amino acids by nasal *Staphylococcus*. (A) Validation of D-amino acid assay to detect D- but no L- stereoisomer amino acids. Significance by one-way ANOVA with Dunnett's posttest; ***p*<0.01 vs LB only control; n = 3 independent experiments **(B)** Clinical CRS-derived methicillin-resistant *S. aureus* (MRSA; strains named beige, white, or silver) or lab strain MRSA M2 increased D-amino acid content in their conditioned media. *S. epidermidis* and methicillin-sensitive *S. aureus* likewise produced D-amino acids. No significant D-amino acid production was observed with clinical *P. aeruginosa* strains 2338, L3847, or P11006 or lab strain PAO1. Significance by one-way ANOVA with Tukey-Kramer posttest; **p*<0.05 for *Staphylococcus* vs *P. aeruginosa*; $^{\#}p$<0.01 vs control; n = 5 independent experiments per bacteria strain. **(C)** CM from patient microbiological cultures predominately containing *S. aureus* produced D-amino acids while those from patients with *P. aeruginosa* did not; n = 3 independent experiments. Significance by one-way ANOVA with Dunnett's posttest; **p*<0.05 vs control (LB only). All bar graphs are mean ± SEM

Figure 5

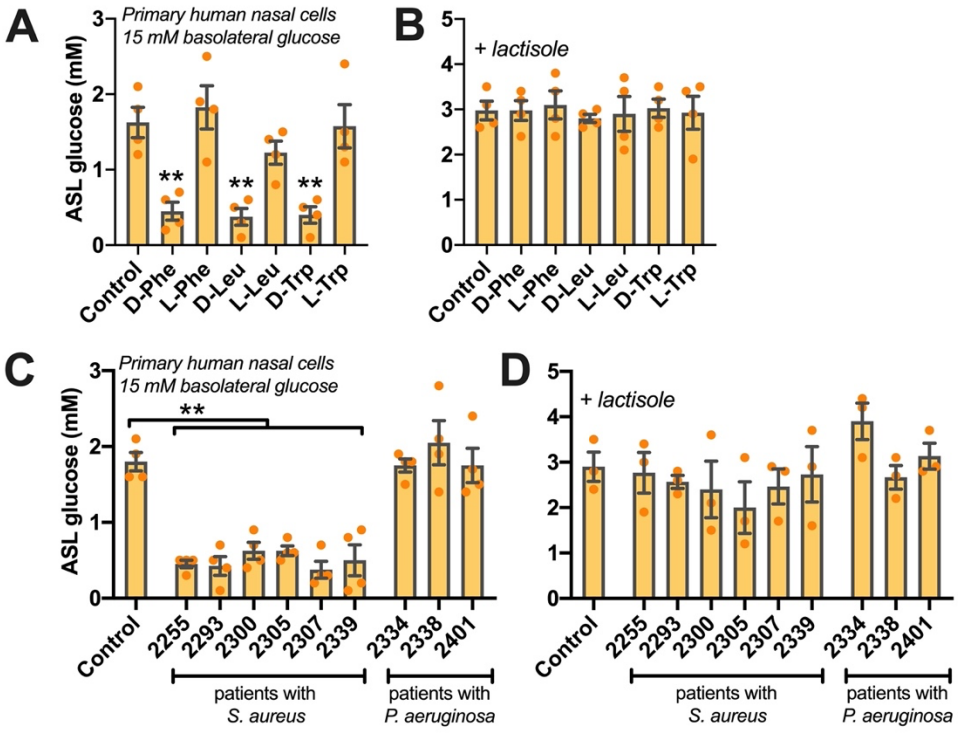

Figure 5. Bacterial D-Amino acids affect ASL glucose levels in a T1R3-dependent manner. (A-B) ASL glucose was measured in 15 mM basolateral glucose to elevate ASL glucose to a measurable range where reductions could reliably be detected. ASL glucose was reduced by D-Phe, D-Leu, or D-Trp (*A*) but not by L-stereoisomers (*A*) or in the presence of T1R3 inhibitor lactisole (*B*). **(C-D)** ASL glucose (15 mM basolateral glucose) was reduced by CM from *S. aureus* patients (C) but not by CM from *P. aeruginosa* patients (*C*) or in the presence of lactisole (*D*). All significance determined by one-way ANOVA with Dunnett's posttest comparing all values to control; $^{**}p<0.01$; n = 4 independent experiments using ALIs from 4 individual patients per condition. All bar graphs show mean ± SEM.

Figure 6

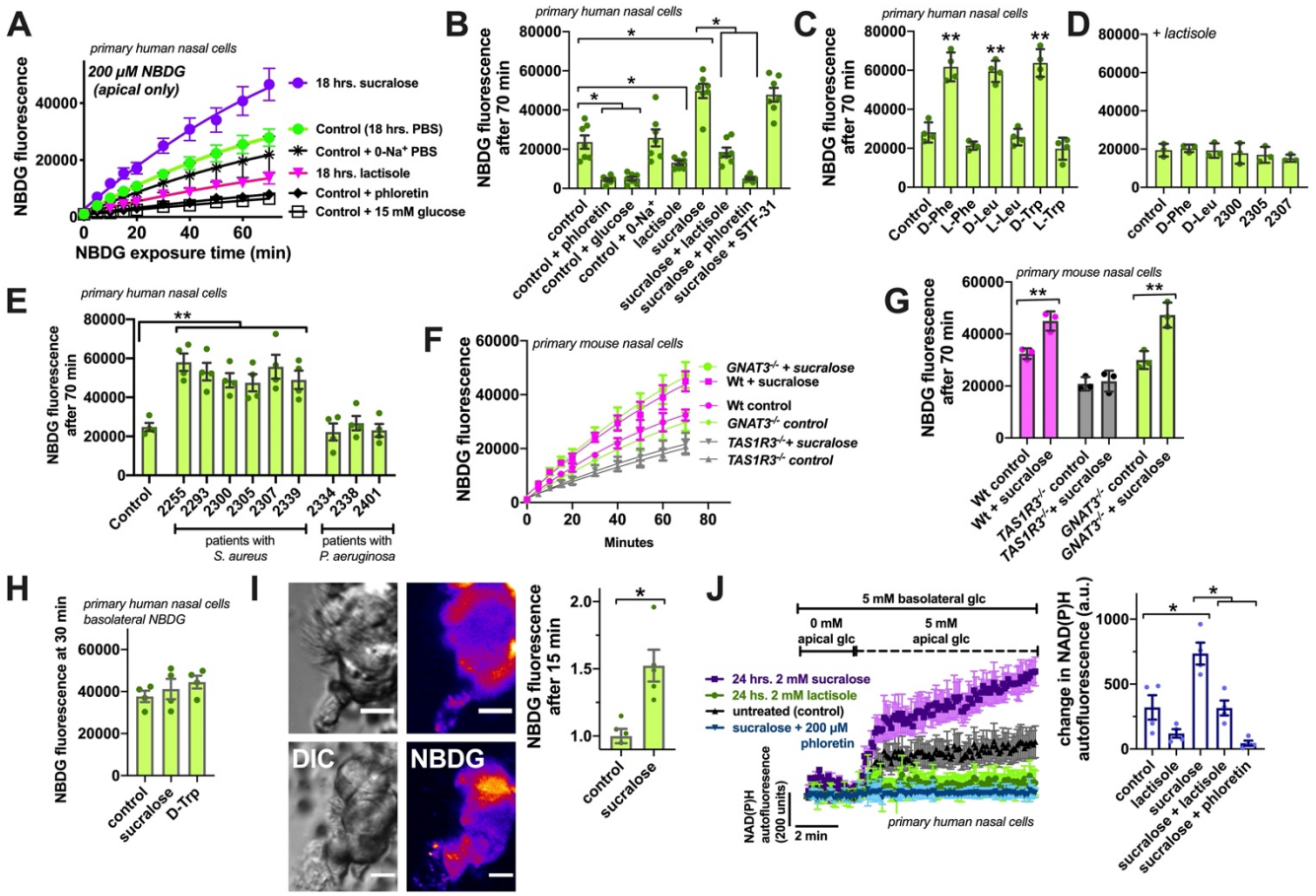

Figure 6. T1R3 regulates apical glucose uptake in nasal epithelial cells. (A) Traces showing uptake of fluorescent NBDG (200 μM; apical side only) in cultures pretreated with sucralose or lactisole or in the acute (beginning of the assay) presence of GLUT inhibitor phloretin, 0-Na^+ PBS, or 15 mM glucose to outcompete the NBDG. **(B)** Quantification of NBDG fluorescence at 70 min from experiments as shown in *A* (n = 7 individual experiments using ALIs derived from 7 patients). Significance determined by one-way ANOVA with Tukey-Kramer posttest; *p<0.05. **(C)** Quantification of apical NBDG uptake at 70 min in the presence of D-isomer or L-isomer amino acids; Significance by one-way ANOVA with Dunnett's posttest comparing all values to control; **p<0.01; n = 4 independent experiments using ALIs from 4 different patients. **(D)** Lactisole reduced the increase in apical NBDG uptake stimulated with D-Phe, D-Leu, or D-Trp. Significance by one-way ANOVA with Dunnett's posttest comparing all values to control + lactisole (all not significantly different); n = 4 independent experiments using ALIs from 4 different patients. **(E)** Bar graph showing increased NBDG fluorescence after 70 min in ALIs exposed to CM from *S. aureus* patients but not *P. aeruginosa* patients. Significance

by one-way ANOVA with Dunnett's posttest comparing all values to control; n = 4 independent experiments using ALIs from 4 different patients; ***p*<0.01. **(F)** Traces of NBDG fluorescence changes in ALIs derived from Wt, *TAS1R3*$^{-/-}$, or *GNAT3*$^{-/-}$ mice ± sucralose. **(G)** Quantification of NBDG fluorescence at 70 min from independent experiments (n = 3) as in F. Sucralose increased apical NBDG uptake in Wt and *GNAT3*$^{-/-}$ mice but not *TAS1R3*$^{-/-}$ mice. Significance by one-way ANOVA with Bonferroni posttest with paired comparisons; ***p*<0.01. **(H)** Bar graph showing lack of difference of basolateral NBDG uptake with sucralose when applied basolateral (n = 4 independent experiments using primary nasal ALIs from 4 separate patients). No significant difference by one-way ANOVA. **(I)** Representative images of NBDG fluorescence uptake in cells acutely isolated from brushings of TRPM5-GFP mice, which labels SCCs. Cell clumps were visually confirmed to lack SCCs prior to the experiment. Bar graph shows relative change in NBDG uptake after 15 min is increased with sucralose, suggesting this is SCC independent. Significance by Student's *t* test; **p*<0.05. **(J)** Left shows representative trace of changes in autofluorescence during addition of 5 mM apical glucose (in PBS) in cells treated with sucralose or lactisole ± acutely applied (at start of assay) GLUT inhibitor phloretin. Bar graph on right shows quantification of increased autofluorescence changes with sucralose and reduction by lactisole or phloretin. Significance by one-way ANOVA with Tukey-Kramer posttest; **p*<0.05.

Figure 7

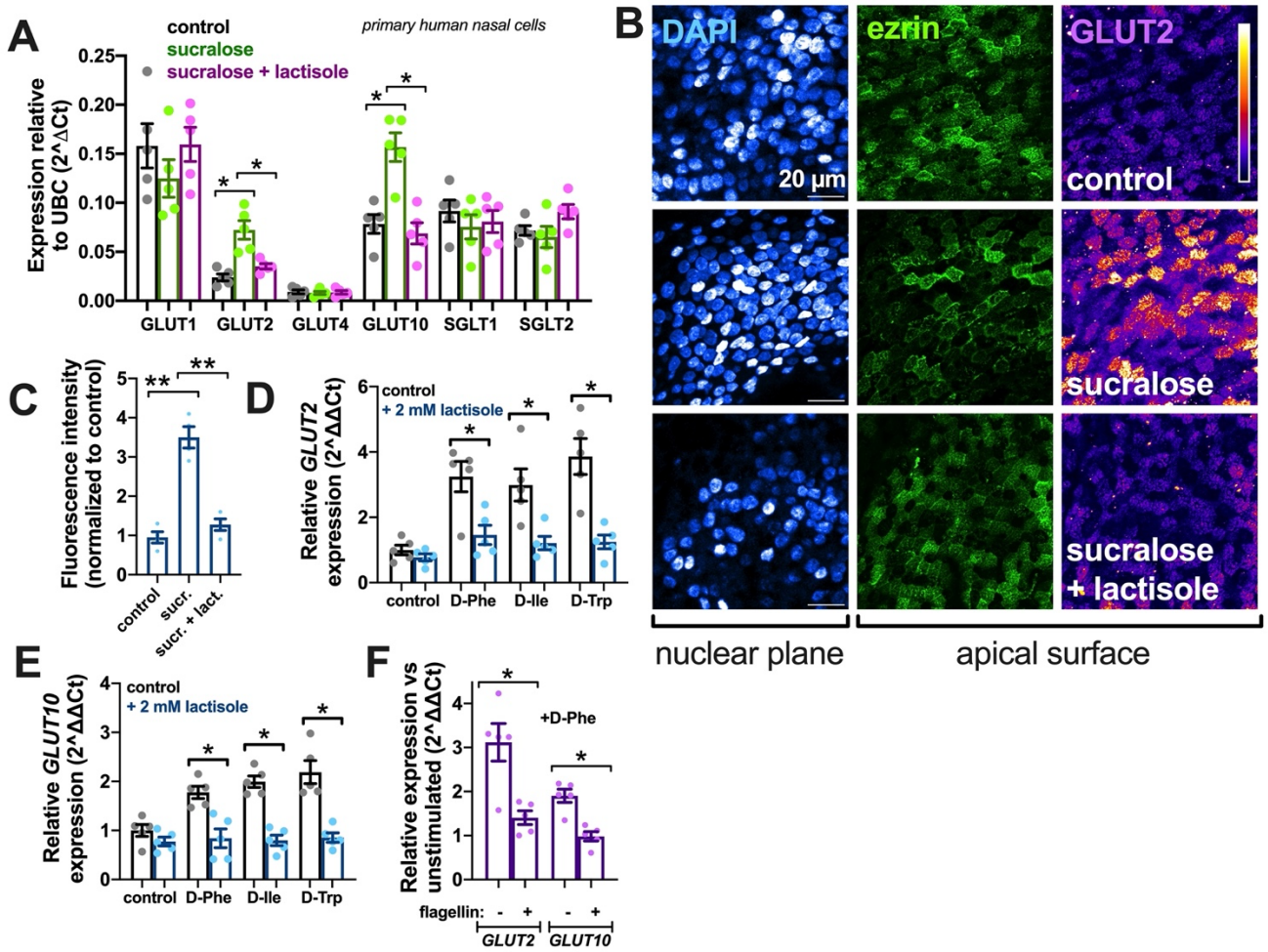

Figure 7. Bacterial D-amino acids increase GLUT2 and GLUT10 expression in a T1R3-dependent manner. (A) Expression of GLUT and SGLT isoform transcripts in cells after stimulation with T1R3 agonist sucralose ± T1R3 inhibitor lactisole in primary nasal ALIs. Significance by one-way ANOVA with Bonferroni posttest comparing expression levels of each gene to control conditions; n = 5 independent experiments using ALIs from 5 separate patients per condition; $p<0.05$. **(B)** Images of ALIs after stimulation with sucralose ± lactisole, showing increased GLUT2 immunofluorescence at the apical membrane (indicated by microvillar marker ezrin). **(C)** Bar graph showing quantification of GLUT2 intensity from 4 independent experiments as in (B) using ALIs from 4 individual patients. Significance by one-way ANOVA with Bonferroni posttest; $^{**}p<0.01$. **(D-E)** Quantification of GLUT2 (*D*) and GLUT10 (*E*) expression (relative to control conditions) after stimulation with sweet D-amino acids ± lactisole. Significance by one-way ANOVA with Bonferroni posttest with pairwise comparisons; $^{*}p<0.05$. **(F)** Relative expression of GLUT2 and GLUT10 after treatment with D-Phe ± TLR5 agonist flagellin. Significance by one-way ANOVA with Bonferroni posttest with pairwise comparisons; $^{*}p<0.05$.

Figure 8

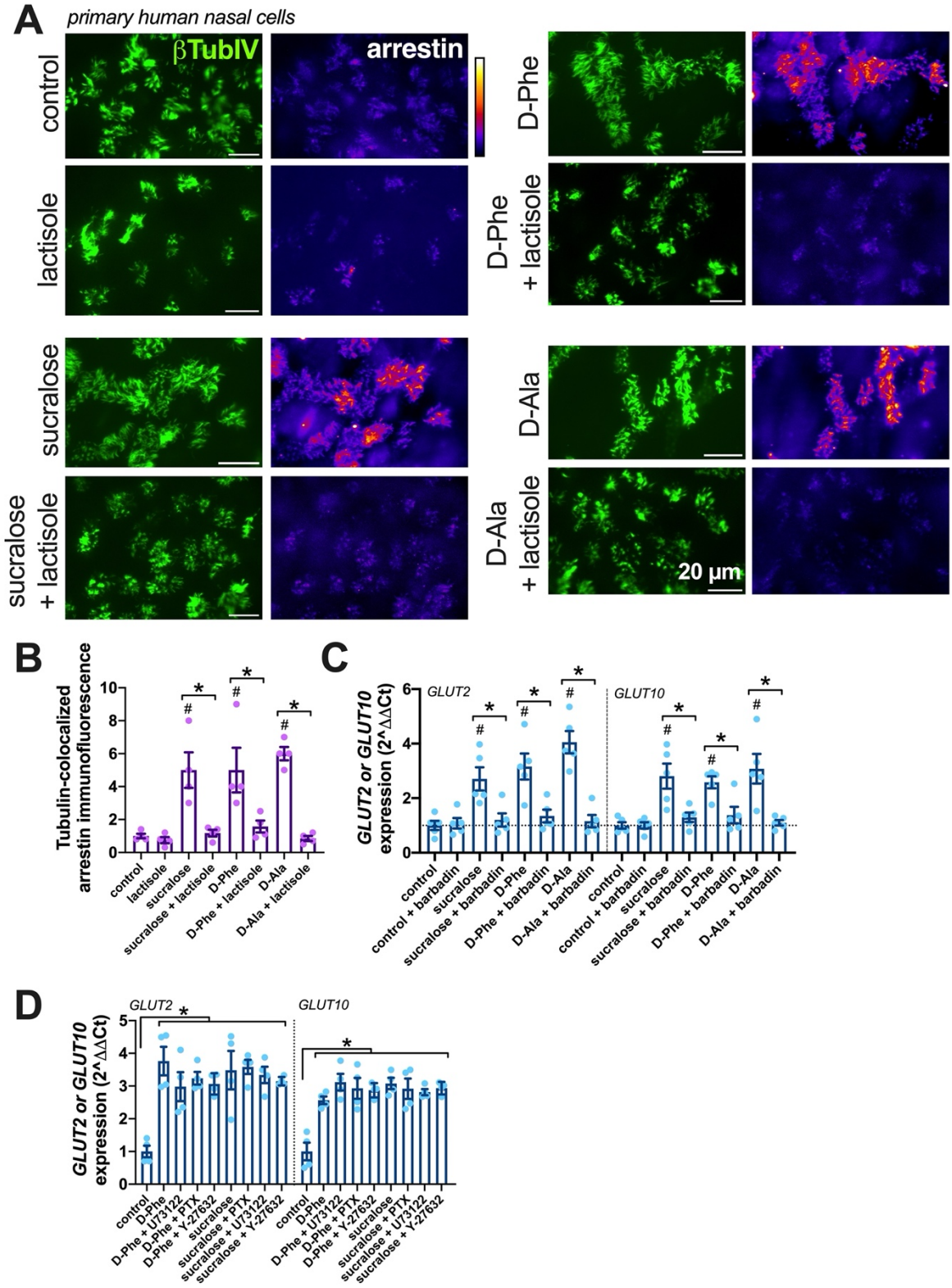
A
primary human nasal cells
βTubIV
arrestin
control
lactisole
sucralose
sucralose + lactisole
D-Phe
D-Phe + lactisole
D-Ala
D-Ala + lactisole
20 µm
B
Tubulin-colocalized arrestin immunofluorescence
control
lactisole
sucralose
sucralose + lactisole
D-Phe
D-Phe + lactisole
D-Ala
D-Ala + lactisole
C
GLUT2 or GLUT10 expression (2^ΔΔCt)
GLUT2
GLUT10
control
control + barbadin
sucralose
sucralose + barbadin
D-Phe
D-Phe + barbadin
D-Ala
D-Ala + barbadin
D
GLUT2 or GLUT10 expression (2^ΔΔCt)
GLUT2
GLUT10
control
D-Phe
D-Phe + U73122
D-Phe + PTX
D-Phe + Y-27632
sucralose
sucralose + PTX
sucralose + U73122
sucralose + Y-27632

Figure 8. T1R3 regulation of GLUT2 and GLUT10 expression likely involves arrestin signaling. **(A)** Immunofluorescence images of primary nasal cilia after stimulation with sweet agonists sucralose, D-Phe, or D-Ala ± lactisole. Cilia marker (β-tubulin IV) and pan-β-arrestin primary antibodies were used. All sets of images taken at identical microscope settings. **(B)** Quantification of cilia-localized (β-tubulin IV-co-localized) arrestin immunofluorescence from 4 independent experiments as in A using cells from 4 separate patients. Significance by one-way ANOVA with Bonferonni posttest comparing all values to control as well as comparing each condition ± lactisole; $^{\#}p<0.05$ vs control; $^{*}p<0.05$ between bracketed bars. **(C)** *GLUT2* and *GLUT10* expression in cultures stimulated with sucralose, D-Phe, or D-Ala ± β-arrestin/β2-adaptin inhibitor barbadin. Significance by one-way ANOVA with Bonferonni posttest comparing all values to control as well as comparing each condition ± barbadin; $^{\#}p<0.05$ vs control; $^{*}p<0.05$ between bracketed bars. **(D)** *GLUT2* and *GLUT10* expression in cultures stimulated with sucralose or D-Phe ± phospholipase C inhibitor U73122, Gαi/Gαgustducin inhibitor pertussis toxin (PTX), or rho kinase inhibitor Y-27632. Significance determined by one-way ANOVA with Bonferroni posttest comparing all values to control or suraclose or D-Phe only as appropriate. Only the control group was significantly different; $^{*}p<0.05$.

References

1. Baker EH, Clark N, Brennan AL, Fisher DA, Gyi KM, Hodson ME, Philips BJ, Baines DL, Wood DM. Hyperglycemia and cystic fibrosis alter respiratory fluid glucose concentrations estimated by breath condensate analysis. J Appl Physiol (1985). 2007;102(5):1969-75. Epub 2007/02/17. doi: 10.1152/japplphysiol.01425.2006. PubMed PMID: 17303703.

2. Baker EH, Baines DL. Airway Glucose Homeostasis: A New Target in the Prevention and Treatment of Pulmonary Infection. Chest. 2018;153(2):507-14. Epub 2017/06/15. doi: 10.1016/j.chest.2017.05.031. PubMed PMID: 28610911.

3. Kalsi KK, Baker EH, Fraser O, Chung YL, Mace OJ, Tarelli E, Philips BJ, Baines DL. Glucose homeostasis across human airway epithelial cell monolayers: role of diffusion, transport and metabolism. Pflugers Arch. 2009;457(5):1061-70. Epub 2008/09/11. doi: 10.1007/s00424-008-0576-4. PubMed PMID: 18781323.

4. Brennan AL, Gyi KM, Wood DM, Johnson J, Holliman R, Baines DL, Philips BJ, Geddes DM, Hodson ME, Baker EH. Airway glucose concentrations and effect on growth of respiratory pathogens in cystic fibrosis. J Cyst Fibros. 2007;6(2):101-9. Epub 2006/07/18. doi: 10.1016/j.jcf.2006.03.009. PubMed PMID: 16844431.

5. Garnett JP, Braun D, McCarthy AJ, Farrant MR, Baker EH, Lindsay JA, Baines DL. Fructose transport-deficient Staphylococcus aureus reveals important role of epithelial glucose transporters in limiting sugar-driven bacterial growth in airway surface liquid. Cell Mol Life Sci. 2014;71(23):4665-73. doi: 10.1007/s00018-014-1635-y. PubMed PMID: 24810961; PMCID: PMC4232747.

6. Garnett JP, Hickman E, Tunkamnerdthai O, Cuthbert AW, Gray MA. Protein phosphatase 1 coordinates CFTR-dependent airway epithelial HCO3- secretion by reciprocal regulation of apical and basolateral membrane Cl(-)-HCO3- exchangers. Br J Pharmacol. 2013;168(8):1946-60. doi: 10.1111/bph.12085. PubMed PMID: 23215877; PMCID: PMC3623064.

7. Garnett JP, Baker EH, Baines DL. Sweet talk: insights into the nature and importance of glucose transport in lung epithelium. Eur Respir J. 2012;40(5):1269-76. Epub 2012/08/11. doi: 09031936.00052612 [pii] 10.1183/09031936.00052612. PubMed PMID: 22878875.

8. Kalsi KK, Baker EH, Medina RA, Rice S, Wood DM, Ratoff JC, Philips BJ, Baines DL. Apical and basolateral localisation of GLUT2 transporters in human lung epithelial cells. Pflugers Arch. 2008;456(5):991-1003. Epub 2008/02/02. doi: 10.1007/s00424-008-0459-8. PubMed PMID: 18239936; PMCID: PMC2480509.

9. Bearham J, Garnett JP, Schroeder V, Biggart MGS, Baines DL. Effective glucose metabolism maintains low intracellular glucose in airway epithelial cells after exposure to hyperglycemia. Am J Physiol Cell Physiol. 2019;317(5):C983-C92. Epub 2019/08/23. doi: 10.1152/ajpcell.00193.2019. PubMed PMID: 31433692; PMCID: PMC6879884.

10. Garnett JP, Nguyen TT, Moffatt JD, Pelham ER, Kalsi KK, Baker EH, Baines DL. Proinflammatory mediators disrupt glucose homeostasis in airway surface liquid. J Immunol. 2012;189(1):373-80. doi: 10.4049/jimmunol.1200718. PubMed PMID: 22623330; PMCID: PMC3605804.

11. Gill SK, Hui K, Farne H, Garnett JP, Baines DL, Moore LS, Holmes AH, Filloux A, Tregoning JS. Increased airway glucose increases airway bacterial load in hyperglycaemia. Sci Rep. 2016;6:27636. doi: 10.1038/srep27636. PubMed PMID: 27273266; PMCID: PMC4897689.

12. Astrand A, Wingren C, Benjamin A, Tregoning JS, Garnett JP, Groves H, Gill S, Orogo-Wenn M, Lundqvist AJ, Walters D, Smith DM, Taylor JD, Baker EH, Baines DL. Dapagliflozin-lowered blood glucose reduces respiratory Pseudomonas aeruginosa infection in diabetic mice. Br J Pharmacol. 2017;174(9):836-47. doi: 10.1111/bph.13741. PubMed PMID: 28192604.

13. Lee RJ, Kofonow JM, Rosen PL, Siebert AP, Chen B, Doghramji L, Xiong G, Adappa ND, Palmer JN, Kennedy DW, Kreindler JL, Margolskee RF, Cohen NA. Bitter and sweet taste receptors regulate human upper respiratory innate immunity. J Clin Invest. 2014;124(3):1393-405. Epub 2014/02/18. doi: 72094 [pii]
10.1172/JCI72094. PubMed PMID: 24531552.

14. Hatten KM, Palmer JN, Lee RJ, Adappa ND, Kennedy DW, Cohen NA. Corticosteroid use does not alter nasal mucus glucose in chronic rhinosinusitis. Otolaryngol Head Neck Surg. 2015;152(6):1140-4. doi: 10.1177/0194599815577567. PubMed PMID: 25820586.

15. Reid L, Meyrick B, Antony VB, Chang LY, Crapo JD, Reynolds HY. The mysterious pulmonary brush cell: a cell in search of a function. Am J Respir Crit Care Med. 2005;172(1):136-9. Epub 2005/04/09. doi: 10.1164/rccm.200502-203WS. PubMed PMID: 15817800; PMCID: PMC2718446.

16. Sell EA, Ortiz-Carpena JF, Herbert DR, Cohen NA. Tuft cells in the pathogenesis of chronic rhinosinusitis with nasal polyps and asthma. Ann Allergy Asthma Immunol. 2021;126(2):143-51. Epub 2020/10/31. doi: 10.1016/j.anai.2020.10.011. PubMed PMID: 33122124; PMCID: PMC8674819.

17. Kohanski MA, Workman AD, Patel NN, Hung LY, Shtraks JP, Chen B, Blasetti M, Doghramji L, Kennedy DW, Adappa ND, Palmer JN, Herbert DR, Cohen NA. Solitary chemosensory cells are a primary epithelial source of IL-25 in patients with chronic rhinosinusitis with nasal polyps. J Allergy Clin Immunol. 2018. Epub 2018/05/21. doi: 10.1016/j.jaci.2018.03.019. PubMed PMID: 29778504.

18. Lee RJ, Hariri BM, McMahon DB, Chen B, Doghramji L, Adappa ND, Palmer JN, Kennedy DW, Jiang P, Margolskee RF, Cohen NA. Bacterial d-amino acids suppress sinonasal innate immunity through sweet taste receptors in solitary chemosensory cells. Sci Signal. 2017;10(495). doi: 10.1126/scisignal.aam7703. PubMed PMID: 28874606.

19. Radkov AD, Moe LA. Bacterial synthesis of D-amino acids. Appl Microbiol Biotechnol. 2014;98(12):5363-74. doi: 10.1007/s00253-014-5726-3. PubMed PMID: 24752840.

20. Sasabe J, Suzuki M. Emerging Role of D-Amino Acid Metabolism in the Innate Defense. Front Microbiol. 2018;9:933. Epub 2018/06/06. doi: 10.3389/fmicb.2018.00933. PubMed PMID: 29867842; PMCID: PMC5954117.

21. Bassoli A, Borgonovo G, Caremoli F, Mancuso G. The taste of D- and L-amino acids: In vitro binding assays with cloned human bitter (TAS2Rs) and sweet (TAS1R2/TAS1R3) receptors. Food Chem. 2014;150:27-33. doi: 10.1016/j.foodchem.2013.10.106. PubMed PMID: 24360415.

22. Merigo F, Benati D, Cristofoletti M, Amaru F, Osculati F, Sbarbati A. Glucose transporter/T1R3-expressing cells in rat tracheal epithelium. J Anat. 2012;221(2):138-50. doi: 10.1111/j.1469-7580.2012.01522.x. PubMed PMID: 22640462; PMCID: 3406361.

23. Kuek LE, Lee RJ. First contact: the role of respiratory cilia in host-pathogen interactions in the airways. Am J Physiol Lung Cell Mol Physiol. 2020;319(4):L603-L19. Epub 2020/08/14. doi: 10.1152/ajplung.00283.2020. PubMed PMID: 32783615.

24. Mao S, Shah AS, Moninger TO, Ostedgaard LS, Lu L, Tang XX, Thornell IM, Reznikov LR, Ernst SE, Karp PH, Tan P, Keshavjee S, Abou Alaiwa MH, Welsh MJ. Motile cilia of human airway epithelia contain hedgehog signaling components that mediate noncanonical hedgehog signaling. Proc

Natl Acad Sci U S A. 2018;115(6):1370-5. Epub 2018/01/24. doi: 10.1073/pnas.1719177115. PubMed PMID: 29358407; PMCID: PMC5819449.

25. Shah AS, Ben-Shahar Y, Moninger TO, Kline JN, Welsh MJ. Motile cilia of human airway epithelia are chemosensory. Science. 2009;325(5944):1131-4. Epub 2009/07/25. doi: 1173869 [pii] 10.1126/science.1173869. PubMed PMID: 19628819.

26. Jain R, Javidan-Nejad C, Alexander-Brett J, Horani A, Cabellon MC, Walter MJ, Brody SL. Sensory functions of motile cilia and implication for bronchiectasis. Front Biosci (Schol Ed). 2012;4:1088-98. Epub 2011/12/29. PubMed PMID: 22202111.

27. Carey RM, Hariri BM, Adappa ND, Palmer JN, Lee RJ. HSP90 Modulates T2R Bitter Taste Receptor Nitric Oxide Production and Innate Immune Responses in Human Airway Epithelial Cells and Macrophages. Cells. 2022;11(9). Epub 2022/05/15. doi: 10.3390/cells11091478. PubMed PMID: 35563784; PMCID: PMC9101439.

28. Carey RM, Lee RJ. Taste Receptors in Upper Airway Innate Immunity. Nutrients. 2019;11(9). Epub 2019/08/31. doi: 10.3390/nu11092017. PubMed PMID: 31466230.

29. Kuek LE, McMahon DB, Ma RZ, Miller ZA, Jolivert JF, Adappa ND, Palmer JN, Lee RJ. Cilia Stimulatory and Antibacterial Activities of T2R Bitter Taste Receptor Agonist Diphenhydramine: Insights into Repurposing Bitter Drugs for Nasal Infections. Pharmaceuticals (Basel). 2022;15(4). Epub 2022/04/24. doi: 10.3390/ph15040452. PubMed PMID: 35455449; PMCID: PMC9025516.

30. Jiang P, Cui M, Zhao B, Snyder LA, Benard LM, Osman R, Max M, Margolskee RF. Identification of the cyclamate interaction site within the transmembrane domain of the human sweet taste receptor subunit T1R3. J Biol Chem. 2005;280(40):34296-305. Epub 2005/08/04. doi: 10.1074/jbc.M505255200. PubMed PMID: 16076846.

31. Cui M, Jiang P, Maillet E, Max M, Margolskee RF, Osman R. The heterodimeric sweet taste receptor has multiple potential ligand binding sites. Curr Pharm Des. 2006;12(35):4591-600. Epub 2006/12/16. PubMed PMID: 17168764.

32. Jiang P, Cui M, Zhao B, Liu Z, Snyder LA, Benard LM, Osman R, Margolskee RF, Max M. Lactisole interacts with the transmembrane domains of human T1R3 to inhibit sweet taste. J Biol Chem. 2005;280(15):15238-46. Epub 2005/01/26. doi: 10.1074/jbc.M414287200. PubMed PMID: 15668251.

33. Sanematsu K, Kusakabe Y, Shigemura N, Hirokawa T, Nakamura S, Imoto T, Ninomiya Y. Molecular Mechanisms for Sweet-suppressing Effect of Gymnemic Acids. J Biol Chem. 2014;289(37):25711-20. doi: 10.1074/jbc.M114.560409. PubMed PMID: 25056955; PMCID: 4162174.

34. Zhao K, Craig JR, Cohen NA, Adappa ND, Khalili S, Palmer JN. Sinus irrigations before and after surgery-Visualization through computational fluid dynamics simulations. Laryngoscope. 2016;126(3):E90-6. Epub 2015/10/16. doi: 10.1002/lary.25666. PubMed PMID: 26467934; PMCID: PMC5084453.

35. Eon Kuek L, Leffler M, Mackay GA, Hulett MD. The MS4A family: counting past 1, 2 and 3. Immunol Cell Biol. 2016;94(1):11-23. Epub 2015/04/04. doi: 10.1038/icb.2015.48. PubMed PMID: 25835430.

36. Damak S, Rong M, Yasumatsu K, Kokrashvili Z, Varadarajan V, Zou S, Jiang P, Ninomiya Y, Margolskee RF. Detection of sweet and umami taste in the absence of taste receptor T1r3. Science. 2003;301(5634):850-3. Epub 2003/07/19. doi: 10.1126/science.1087155. PubMed PMID: 12869700.

37. Schiffman SS, Sennewald K, Gagnon J. Comparison of taste qualities and thresholds of D- and L-amino acids. Physiol Behav. 1981;27(1):51-9. PubMed PMID: 7267802.

38. Solms J, Vuataz L, Egli RH. The taste of L- and D-amino acids. Experientia. 1965;21(12):692-4. PubMed PMID: 5869699.

39. Harro JM, Daugherty S, Bruno VM, Jabra-Rizk MA, Rasko DA, Shirtliff ME. Draft Genome Sequence of the Methicillin-Resistant Staphylococcus aureus Isolate MRSA-M2. Genome Announc. 2013;1(1). doi: 10.1128/genomeA.00037-12. PubMed PMID: 23405318; PMCID: PMC3569307.

40. Lam H, Oh DC, Cava F, Takacs CN, Clardy J, de Pedro MA, Waldor MK. D-amino acids govern stationary phase cell wall remodeling in bacteria. Science. 2009;325(5947):1552-5. doi: 10.1126/science.1178123. PubMed PMID: 19762646; PMCID: 2759711.

41. Yamada K, Nakata M, Horimoto N, Saito M, Matsuoka H, Inagaki N. Measurement of glucose uptake and intracellular calcium concentration in single, living pancreatic beta-cells. J Biol Chem. 2000;275(29):22278-83. doi: 10.1074/jbc.M908048199. PubMed PMID: 10748091.

42. Yamada K, Saito M, Matsuoka H, Inagaki N. A real-time method of imaging glucose uptake in single, living mammalian cells. Nat Protoc. 2007;2(3):753-62. doi: 10.1038/nprot.2007.76. PubMed PMID: 17406637.

43. Clapp TR, Medler KF, Damak S, Margolskee RF, Kinnamon SC. Mouse taste cells with G protein-coupled taste receptors lack voltage-gated calcium channels and SNAP-25. BMC Biol. 2006;4:7. Epub 2006/04/01. doi: 10.1186/1741-7007-4-7. PubMed PMID: 16573824; PMCID: 1444931.

44. Gulbransen BD, Clapp TR, Finger TE, Kinnamon SC. Nasal solitary chemoreceptor cell responses to bitter and trigeminal stimulants in vitro. J Neurophysiol. 2008;99(6):2929-37. Epub 2008/04/18. doi: 00066.2008 [pii]
10.1152/jn.00066.2008. PubMed PMID: 18417634.

45. Bartolome F, Abramov AY. Measurement of mitochondrial NADH and FAD autofluorescence in live cells. Methods Mol Biol. 2015;1264:263-70. Epub 2015/01/30. doi: 10.1007/978-1-4939-2257-4_23. PubMed PMID: 25631020.

46. Blacker TS, Duchen MR. Investigating mitochondrial redox state using NADH and NADPH autofluorescence. Free Radic Biol Med. 2016. doi: 10.1016/j.freeradbiomed.2016.08.010. PubMed PMID: 27519271.

47. Segade F. Glucose transporter 10 and arterial tortuosity syndrome: the vitamin C connection. FEBS Lett. 2010;584(14):2990-4. Epub 2010/06/16. doi: 10.1016/j.febslet.2010.06.011. PubMed PMID: 20547159.

48. Dawson PA, Mychaleckyj JC, Fossey SC, Mihic SJ, Craddock AL, Bowden DW. Sequence and functional analysis of GLUT10: a glucose transporter in the Type 2 diabetes-linked region of chromosome 20q12-13.1. Mol Genet Metab. 2001;74(1-2):186-99. Epub 2001/10/11. doi: 10.1006/mgme.2001.3212. PubMed PMID: 11592815.

49. McVie-Wylie AJ, Lamson DR, Chen YT. Molecular cloning of a novel member of the GLUT family of transporters, SLC2a10 (GLUT10), localized on chromosome 20q13.1: a candidate gene for NIDDM susceptibility. Genomics. 2001;72(1):113-7. Epub 2001/03/15. doi: 10.1006/geno.2000.6457. PubMed PMID: 11247674.

50. Lee RJ, Xiong G, Kofonow JM, Chen B, Lysenko A, Jiang P, Abraham V, Doghramji L, Adappa ND, Palmer JN, Kennedy DW, Beauchamp GK, Doulias P-T, Ischiropoulos H, Kreindler JL, Reed DR,

Cohen NA. T2R38 taste receptor polymorphisms underlie susceptibility to upper respiratory infection. J Clin Invest. 2012;122(11):4145-59.

51. Guerra ML, Kalwat MA, McGlynn K, Cobb MH. Sucralose activates an ERK1/2-ribosomal protein S6 signaling axis. FEBS Open Bio. 2017;7(2):174-86. doi: 10.1002/2211-5463.12172. PubMed PMID: 28174684; PMCID: PMC5292669.

52. Beautrait A, Paradis JS, Zimmerman B, Giubilaro J, Nikolajev L, Armando S, Kobayashi H, Yamani L, Namkung Y, Heydenreich FM, Khoury E, Audet M, Roux PP, Veprintsev DB, Laporte SA, Bouvier M. A new inhibitor of the beta-arrestin/AP2 endocytic complex reveals interplay between GPCR internalization and signalling. Nat Commun. 2017;8:15054. Epub 2017/04/19. doi: 10.1038/ncomms15054. PubMed PMID: 28416805; PMCID: PMC5399295.

53. Max M, Shanker YG, Huang L, Rong M, Liu Z, Campagne F, Weinstein H, Damak S, Margolskee RF. Tas1r3, encoding a new candidate taste receptor, is allelic to the sweet responsiveness locus Sac. Nat Genet. 2001;28(1):58-63. Epub 2001/04/28. doi: 10.1038/88270. PubMed PMID: 11326277.

54. Nelson G, Hoon MA, Chandrashekar J, Zhang Y, Ryba NJ, Zuker CS. Mammalian sweet taste receptors. Cell. 2001;106(3):381-90. Epub 2001/08/18. PubMed PMID: 11509186.

55. Li X, Staszewski L, Xu H, Durick K, Zoller M, Adler E. Human receptors for sweet and umami taste. Proc Natl Acad Sci U S A. 2002;99(7):4692-6. Epub 2002/03/28. doi: 10.1073/pnas.072090199 072090199 [pii]. PubMed PMID: 11917125.

56. Kojima I, Nakagawa Y, Ohtsu Y, Medina A, Nagasawa M. Sweet Taste-Sensing Receptors Expressed in Pancreatic beta-Cells: Sweet Molecules Act as Biased Agonists. Endocrinol Metab (Seoul). 2014;29(1):12-9. Epub 2014/04/18. doi: 10.3803/EnM.2014.29.1.12. PubMed PMID: 24741449; PMCID: 3970274.

57. Nakagawa Y, Ohtsu Y, Nagasawa M, Shibata H, Kojima I. Glucose promotes its own metabolism by acting on the cell-surface glucose-sensing receptor T1R3. Endocr J. 2014;61(2):119-31. Epub 2013/11/10. PubMed PMID: 24200979.

58. Medina A, Nakagawa Y, Ma J, Li L, Hamano K, Akimoto T, Ninomiya Y, Kojima I. Expression of the glucose-sensing receptor T1R3 in pancreatic islet: changes in the expression levels in various nutritional and metabolic states. Endocr J. 2014. Epub 2014/06/06. PubMed PMID: 24898279.

59. Nie Y, Vigues S, Hobbs JR, Conn GL, Munger SD. Distinct contributions of T1R2 and T1R3 taste receptor subunits to the detection of sweet stimuli. Curr Biol. 2005;15(21):1948-52. Epub 2005/11/08. doi: 10.1016/j.cub.2005.09.037. PubMed PMID: 16271873.

60. Maitrepierre E, Sigoillot M, Le Pessot L, Briand L. Recombinant expression, in vitro refolding, and biophysical characterization of the N-terminal domain of T1R3 taste receptor. Protein Expr Purif. 2012;83(1):75-83. Epub 2012/03/28. doi: 10.1016/j.pep.2012.03.006. PubMed PMID: 22450161.

61. Kim SK, Chen Y, Abrol R, Goddard WA, 3rd, Guthrie B. Activation mechanism of the G protein-coupled sweet receptor heterodimer with sweeteners and allosteric agonists. Proc Natl Acad Sci U S A. 2017;114(10):2568-73. Epub 2017/02/24. doi: 10.1073/pnas.1700001114. PubMed PMID: 28228527; PMCID: PMC5347580.

62. Maillet EL, Cui M, Jiang P, Mezei M, Hecht E, Quijada J, Margolskee RF, Osman R, Max M. Characterization of the Binding Site of Aspartame in the Human Sweet Taste Receptor. Chem Senses. 2015;40(8):577-86. Epub 2015/09/18. doi: 10.1093/chemse/bjv045. PubMed PMID: 26377607; PMCID: PMC4675835.

63. Belloir C, Brule M, Tornier L, Neiers F, Briand L. Biophysical and functional characterization of the human TAS1R2 sweet taste receptor overexpressed in a HEK293S inducible cell line. Sci Rep. 2021;11(1):22238. Epub 2021/11/17. doi: 10.1038/s41598-021-01731-3. PubMed PMID: 34782704; PMCID: PMC8593021.

64. Mahalapbutr P, Darai N, Panman W, Opasmahakul A, Kungwan N, Hannongbua S, Rungrotmongkol T. Atomistic mechanisms underlying the activation of the G protein-coupled sweet receptor heterodimer by sugar alcohol recognition. Sci Rep. 2019;9(1):10205. Epub 2019/07/17. doi: 10.1038/s41598-019-46668-w. PubMed PMID: 31308429; PMCID: PMC6629994.

65. Bachmanov AA, Tordoff MG, Beauchamp GK. Sweetener preference of C57BL/6ByJ and 129P3/J mice. Chem Senses. 2001;26(7):905-13. Epub 2001/09/14. doi: 10.1093/chemse/26.7.905. PubMed PMID: 11555485; PMCID: PMC3718299.

66. Lossow K, Hubner S, Roudnitzky N, Slack JP, Pollastro F, Behrens M, Meyerhof W. Comprehensive Analysis of Mouse Bitter Taste Receptors Reveals Different Molecular Receptive Ranges for Orthologous Receptors in Mice and Humans. J Biol Chem. 2016;291(29):15358-77. doi: 10.1074/jbc.M116.718544. PubMed PMID: 27226572; PMCID: PMC4946946.

67. Bren A, Park JO, Towbin BD, Dekel E, Rabinowitz JD, Alon U. Glucose becomes one of the worst carbon sources for E.coli on poor nitrogen sources due to suboptimal levels of cAMP. Sci Rep. 2016;6:24834. Epub 2016/04/26. doi: 10.1038/srep24834. PubMed PMID: 27109914; PMCID: PMC4843011.

68. Vitko NP, Grosser MR, Khatri D, Lance TR, Richardson AR. Expanded Glucose Import Capability Affords Staphylococcus aureus Optimized Glycolytic Flux during Infection. mBio. 2016;7(3). Epub 2016/06/23. doi: 10.1128/mBio.00296-16. PubMed PMID: 27329749; PMCID: PMC4916373.

69. Luo Z, Yue S, Chen T, She P, Wu Y, Wu Y. Reduced Growth of Staphylococcus aureus Under High Glucose Conditions Is Associated With Decreased Pentaglycine Expression. Front Microbiol. 2020;11:537290. Epub 2020/11/24. doi: 10.3389/fmicb.2020.537290. PubMed PMID: 33224107; PMCID: PMC7667020.

70. Stevens WW, Lee RJ, Schleimer RP, Cohen NA. Chronic rhinosinusitis pathogenesis. J Allergy Clin Immunol. 2015;136(6):1442-53. doi: 10.1016/j.jaci.2015.10.009. PubMed PMID: 26654193; PMCID: PMC4680986.

71. Hariri BM, McMahon DB, Chen B, Adappa ND, Palmer JN, Kennedy DW, Lee RJ. Plant flavones enhance antimicrobial activity of respiratory epithelial cell secretions against Pseudomonas aeruginosa. PLoS One. 2017;12(9):e0185203. doi: 10.1371/journal.pone.0185203. PubMed PMID: 28931063; PMCID: PMC5607194.

72. Hariri BM, McMahon DB, Chen B, Freund JR, Mansfield CJ, Doghramji LJ, Adappa ND, Palmer JN, Kennedy DW, Reed DR, Jiang P, Lee RJ. Flavones modulate respiratory epithelial innate immunity: anti-inflammatory effects and activation of the T2R14 receptor. J Biol Chem. 2017;292(20):8484-97. Epub Apr 3. doi: 10.1074/jbc.M116.771949. PubMed PMID: 28373278.

73. McMahon DB, Workman AD, Kohanski MA, Carey RM, Freund JR, Hariri BM, Chen B, Doghramji LJ, Adappa ND, Palmer JN, Kennedy DW, Lee RJ. Protease-activated receptor 2 activates airway apical membrane chloride permeability and increases ciliary beating. FASEB J. 2018;32(1):155-67. doi: 10.1096/fj.201700114RRR. PubMed PMID: 28874459.

74. Freund JR, Mansfield CJ, Doghramji LJ, Adappa ND, Palmer JN, Kennedy DW, Reed DR, Jiang P, Lee RJ. Activation of airway epithelial bitter taste receptors by Pseudomonas aeruginosa quinolones modulates calcium, cyclic-AMP, and nitric oxide signaling. J Biol Chem. 2018;293(25):9824-40. Epub 2018/05/12. doi: 10.1074/jbc.RA117.001005. PubMed PMID: 29748385; PMCID: PMC6016477.

75. Lee RJ, Chen B, Redding KM, Margolskee RF, Cohen NA. Mouse nasal epithelial innate immune responses to Pseudomonas aeruginosa quorum-sensing molecules require taste signaling components. Innate Immun. 2014;20(6):606-17. Epub 2013/09/21. doi: 10.1177/1753425913503386. PubMed PMID: 24045336.

76. Schindelin J, Arganda-Carreras I, Frise E, Kaynig V, Longair M, Pietzsch T, Preibisch S, Rueden C, Saalfeld S, Schmid B, Tinevez JY, White DJ, Hartenstein V, Eliceiri K, Tomancak P, Cardona A. Fiji: an open-source platform for biological-image analysis. Nat Methods. 2012;9(7):676-82. doi: 10.1038/nmeth.2019. PubMed PMID: 22743772; PMCID: PMC3855844.

77. Gopallawa I, Freund JR, Lee RJ. Bitter taste receptors stimulate phagocytosis in human macrophages through calcium, nitric oxide, and cyclic-GMP signaling. Cell Mol Life Sci. 2021;78(1):271-86. Epub 2020/03/17. doi: 10.1007/s00018-020-03494-y. PubMed PMID: 32172302; PMCID: PMC7492447.

78. McMahon DB, Kuek LE, Johnson ME, Johnson PO, Horn RLJ, Carey RM, Adappa ND, Palmer JN, Lee RJ. The bitter end: T2R bitter receptor agonists elevate nuclear calcium and induce apoptosis in non-ciliated airway epithelial cells. Cell Calcium. 2022;101:102499. Epub 2021/11/29. doi: 10.1016/j.ceca.2021.102499. PubMed PMID: 34839223; PMCID: PMC8752513.